Dynamics of a filtered-feedback laser: influence of the filter width

Hartmut Erzgräber[1,*] and Bernd Krauskopf[2]

[1]*School of Mathematical Sciences, Queen Mary, University of London, London E1 4NS, UK*
[2]*Department of Engineering Mathematics, Queen's Building, University of Bristol, Bristol BS8 1TR, UK*
[*]*Corresponding author: h.erzgraeber@qmul.ac.uk*

Received May 17, 2007; accepted July 9, 2007;
posted July 17, 2007 (Doc. ID 83147); published August 9, 2007

The behavior of a semiconductor laser subject to filtered optical feedback is studied in dependence on the width of the filter. Of special interest are pure frequency oscillations where the laser intensity is practically constant. We show that frequency oscillations are stable in a large region of intermediate values of the filter width, where the dispersion of the filter is able to compensate for the well-known phase-amplitude coupling of the semiconductor laser. Our stability diagram covers the entire range from a very narrow filter, when the system behaves like a laser with monochromatic optical injection, to a very broad filter, when the laser effectively receives conventional (i.e., unfiltered) optical feedback. © 2007 Optical Society of America

OCIS codes: 140.5960, 190.3100, 000.4430.

We consider a semiconductor laser with filtered optical feedback (FOF), where a part of the laser light is spectrally filtered and reinjected into the laser after the round-trip time τ of the feedback loop. In an experimental setup spectral filtering can be realized, for example, by a Fabry–Perot interferometer where optical isolators prevent unwanted reflections; see Fig. 1. The filter itself is characterized by the detuning Δ between the laser frequency and the filter center frequency, and by the filter width Λ. These two parameters offer additional control over the feedback light, which may be used to influence the dynamics of the laser; see also, for example, [1–4] for other optical feedback schemes.

The dynamics of the FOF laser has been considered in a number of experimental and theoretical studies; see, for example, [5–8]. Their focus has been on the influence of the detuning, the feedback strength, and the external round-trip time. By contrast, studies of the influence of the filter width Λ have focused so far on the two limiting cases of an extremely narrow filter and of an extremely broad filter. Namely, the narrow-filter limit reduces to a laser with optically injected light at the filter frequency, while in the broad-filter limit spectral filtering is lost so that the system reduces to a laser with conventional optical feedback [9–11]; in both limits spectral filtering can be neglected. However, in a real system where the feedback light is subject to spectral filtering, intermediate filter widths are of interest.

In this paper we study how the behavior of the FOF laser is influenced by the filter width Λ over several orders of magnitude, ranging from zero up to 4 GHz. This is motivated by recent experimental measurements in [12], where the vital influence of Λ in an intermediate range was revealed by changing the distance between the two mirrors of the Fabry–Perot interferometer. Of special interest are frequency oscillations (FOs) of the system, which are characterized by an absence of oscillations of the power of the laser. In this respect FOs are very different from the well-known relaxation oscillations (ROs) that are a typical feature of semiconductor lasers. In fact, in light of the strong amplitude–phase coupling of semiconductor lasers, the existence of FOs in the FOF laser—first reported in [6]—has been somewhat surprising. Their existence has been explained by the influence of the filter dispersion, which effectively compensates for the dynamics in the laser intensity [8]. It is therefore natural to ask in which range of the filter width Λ stable FOs can be found.

Specifically, we identify stability regions of different types of dynamics by means of a bifurcation analysis of an established rate equation model [8]. It describes the evolution of the complex-valued envelope $E(t)$ of the laser field, the real-valued laser inversion $N(t)$, and the complex-valued envelope $F(t)$ of the feedback field. The model can be written in dimensionless form as

$$\dot{E} = (1 + i\alpha)N(t)E(t) + \kappa F(t), \tag{1}$$

$$T\dot{N} = P - N(t) - (1 + 2N(t))|E(t)|^2, \tag{2}$$

$$\dot{F} = \Lambda E(t - \tau)e^{-iC_p} + (i\Delta - \Lambda)F(t). \tag{3}$$

The feedback field is modeled by Eq. (3), where the profile of the Fabry–Perot filter is approximated by a single Lorentzian with width (half-width at half-maximum) Λ and detuning Δ. The filtered field F enters the laser field E after the delay time τ with feed-

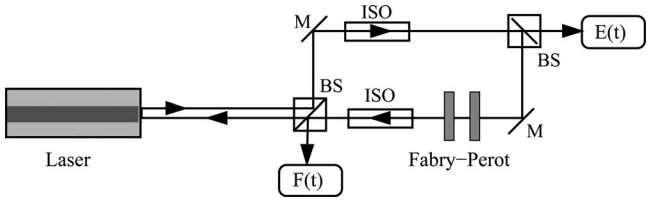

Fig. 1. Sketch of the FOF laser system with a semiconductor laser, Fabry–Perot filter, beam splitter (BS), optical isolators (ISO), and mirrors (M).

0146-9592/07/162441-3/$15.00

back strength κ, where the feedback phase C_p describes the exact phase relationship between the two fields. Standard semiconductor laser parameters are the linewidth enhancement factor α, the (rescaled) carrier lifetime T, and the pump rate P. Note that time t is measured in units of the photon decay time of the laser, which is 10 ps for a typical semiconductor laser. In the normalization of Eqs. (1)–(3) we choose the realistic values $\alpha=5.0$, $T=100$, $P=2.55$, $\tau=743$, $\kappa=0.0127$, and $\Delta=-0.042$. In physical terms, this corresponds to a laser that is pumped 1.6 times above threshold and receives filtered light of a detuning of −0.67 GHz (i.e., the filter center is on the blue side with respect to the solitary laser frequency) after a delay time of 7.43 ns (equivalent to a feedback loop of about 2.2 m length).

To analyze Eqs. (1)–(3) we use numerical continuation techniques [13,14] that allow one to find and follow solutions in parameters and to determine their stability properties; see also [15]. In this way, we are able to provide a comprehensive overview of the stability and the dynamics of the system when the filter width Λ is allowed to vary over its entire range. In this study it is advantageous to allow the feedback phase C_p to vary, because it has been identified as an important parameter for the FOF laser [8] and is crucial in the limiting case of $\Lambda\to 0$ [10].

Figure 2 shows a typical example of FOs (thick curve), together with the external filtered modes (EFMs, thin curve), in projection onto the (ν,I_L) plane and the (ν,I_F) plane for $\Lambda=0.34$ GHz and $C_p=0$. The advantage of the projection onto the (ν,I_F) plane in Fig. 2(b) is that it shows the role of the filter for pure FOs. The EFMs are the basic solutions of Eqs. (1)–(3), and they correspond to cw emission of the form

$$(E(t);N(t);F(t)) = (\sqrt{I_L}e^{i\omega_s t};N_s;\sqrt{I_F}e^{i\omega_s t+i\phi})$$

with constant intensities I_L and I_F of the laser and the feedback field, respectively, and constant inversion N_s, frequency ω_s, and phase shift ϕ. The EFMs form a single closed curve, called an EFM component, as the feedback phase C_p is changed. For the chosen values of the parameters there are 19 EFMs, marked by squares (when stable) and circles (when unstable). Figure 2(a) shows the usual representation of the EFM component in the (ν,I_L) plane, which is often referred to as the fixed point ellipse; compare with [5]. In Fig. 2(b), on the other hand, the shape of the EFM component reflects the dispersion characteristics of the filter. That is, the feedback intensity is highest for EFMs close to the filter center, and it decreases for EFMs toward the flanks of the filter. It can be seen clearly that the periodic FO orbit indeed occurs at and involves the flank of the filter. This means that any change of the laser frequency ν results in a change of the feedback intensity I_F, while the laser intensity I_L remains practically constant. This property of FOs indicates that they can be maintained only at an intermediate range of filter widths and must disappear when the filter width becomes too broad or too narrow.

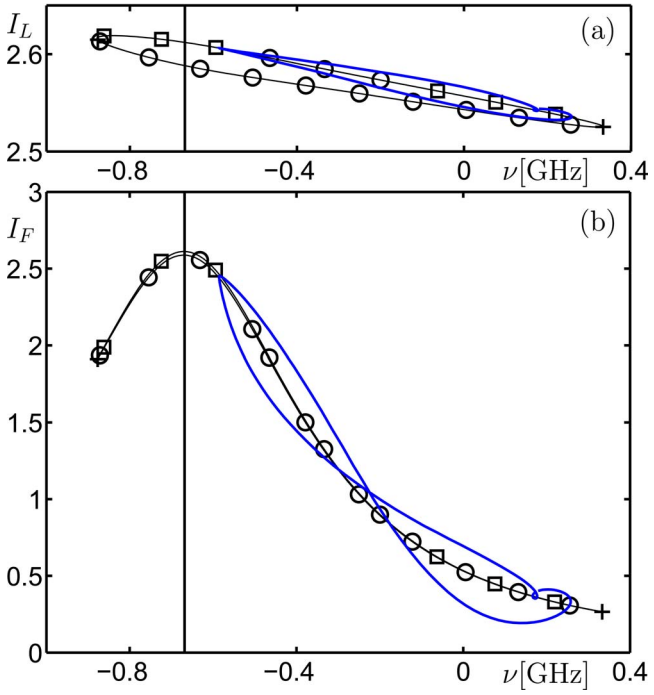

Fig. 2. (Color online) Periodic orbit (thick curve) of stable FOs for $\Lambda=0.34$ GHz and $C_p=0$ in projection onto the (ν,I_L) plane (a) and onto the (ν,I_F) plane (b); notice the different scales along the vertical axes. Stable (squares) and unstable (circles) EFMs lie on a closed (thin) curve (as a function of C_p); the vertical line indicates the center frequency of the filter.

We now take a more global view and show in Fig. 3 stability regions of EFM, FOs, and ROs of the FOF laser in the (Λ,C_p) plane over a large range of Λ and over several periods of the 2π-periodic parameter C_p. This representation is more convenient than plotting the information in only a single 2π interval of C_p; see [8] for a discussion of the multistability resulting from the 2π periodicity.

The stability region of the EFMs is labeled as such in Fig. 3; at least one EFM always exists. Additional EFMs are born in pairs in saddle-node bifurcations (S) as the filter width Λ or the feedback phase C_p is changed; one of them is stable in the EFM region.

In particular, when C_p is changed for $\Lambda<0.1$, two seemingly unconnected stable EFM regions are observed that are separated by the white area to the left of the saddle-node curve S in Fig. 3. The EFM region centered around $C_p=-5\pi$ corresponds to EFMs near the solitary laser frequency, and the one centered around $C_p=4\pi$ corresponds to EFMs near the center frequency of the filter. However, for Λ above about 0.1 these two regions are connected and form a single stable EFM region.

We now concentrate on bifurcating oscillations that arise when EFMs become unstable at (supercritical) Hopf bifurcations (H). Figure 3 shows a region of stable FOs for values of Λ below 0.5 GHz and a disjoint region of stable ROs for $\Lambda>1$ GHz. Both stability regions are bounded by curves of further bifurcations; we find torus bifurcations (T), period-doubling bifurcations (PD), and saddle node of limit cycle bifurcations (SL). Note that these bifurcations may

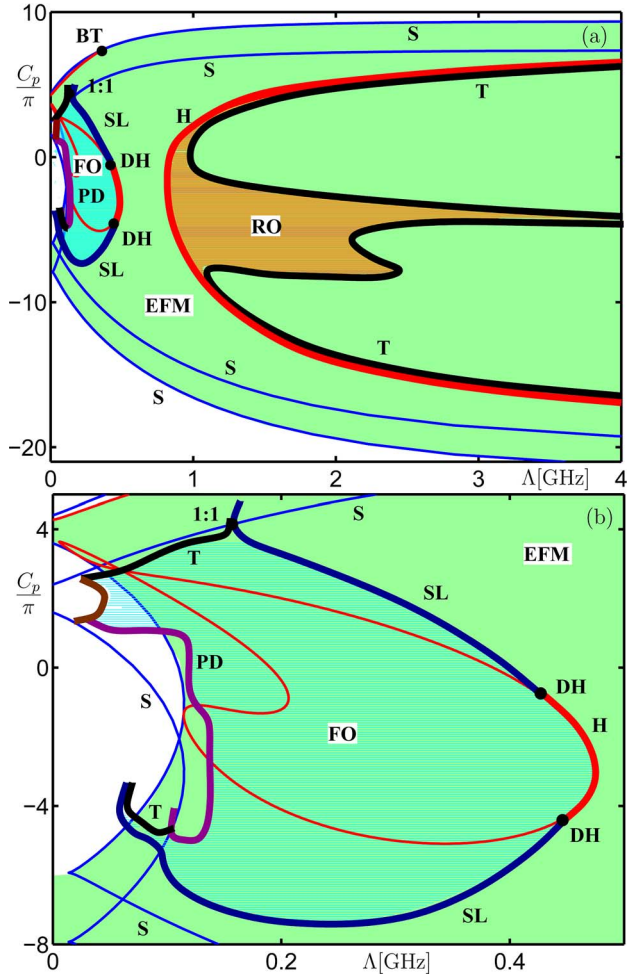

Fig. 3. (Color online) Stability regions of EFMs, ROs, and FOs in the (Λ, C_p) plane (a) and an enlarged view near the FO region (b). Boundary curves are given by saddle-node bifurcations (S), Hopf bifurcations (H), saddle-node bifurcations of limit cycles (SL), torus bifurcations (T), and period-doubling bifurcation (PD); the short curve near C_p indicates a more complicated transition from stable FOs.

give rise to more complicated dynamics, which are beyond the scope of this Letter.

As can be seen from Fig. 3(a), ROs can be found for rather higher values of the filter width Λ. They are due to a weakly damped internal instability of semiconductor lasers that may undamp under the influence of any external perturbation, such as sufficiently strong feedback. Note that ROs can be found near the frequency of the filter irrespective of the value of the detuning; compare this also with [8]. The undamping of the ROs is common for lasers with any type of optical feedback and does not require filtering. This is why ROs occur for a rather large filter width, where the filter has only little effect on the feedback light across the frequency range of the laser.

Frequency oscillations, on the other hand, occur in a stability region, enlarged in Fig. 3(b), for intermediate values of the filter width Λ. When entering the stability region by decreasing Λ, FOs are born from the stable EFM in a supercritical Hopf bifurcation (H) or in pairs in a saddle node of limit cycle bifurcations (SL). In the stability region of FOs the filter indeed has an appropriate flank, which agrees with our earlier observation; see Fig. 2(b). When the filter becomes too narrow, the dispersion can no longer compensate the phase-amplitude coupling of the laser and the FOs lose their stability. This may occur in period-doubling (PD) or torus (T) bifurcations. Moreover, we find a complicated bifurcation scenario involving homoclinic connections when leaving the EFM stability area near $C_p \sim 2\pi$.

In conclusion, we provided a comprehensive picture of how the dynamics of a semiconductor laser with filtered optical feedback depends on the filter width. This revealed that frequency oscillations, which require dispersion at the filter flank, occur stably in a region of intermediate filter width. Relaxation oscillations, on the other hand, occur for much wider filters. This distinction between the two types of oscillations may prove useful for possible applications of laser systems with filtering elements.

References

1. F. Mogensen, H. Olesen, and G. Jacobsen, IEEE J. Quantum Electron. **QE-21**, 784 (1985).
2. F. Rogister, P. Mégret, O. Deparis, M. Blondel, and T. Erneux, Opt. Lett. **24**, 1218 (1999).
3. S. Mandre, I. Fischer, and W. Elsäßer, Opt. Lett. **28**, 1135 (2003).
4. V. Tronciu, H.-J. Wünsche, M. Wolfrum, and M. Radziunas, Phys. Rev. E **73**, 046205 (2006).
5. M. Yousefi and D. Lenstra, IEEE J. Quantum Electron. **35**, 970 (1999).
6. A. Fischer, O. Andersen, M. Yousefi, S. Stolte, and D. Lenstra, IEEE J. Quantum Electron. **36**, 375 (2000).
7. A. Fischer, M. Yousefi, D. Lenstra, M. Carter, and G. Vemuri, Phys. Rev. Lett. **92**, 023901 (2004).
8. H. Erzgräber, B. Krauskopf, and D. Lenstra, SIAM J. Appl. Dyn. Syst. **6**, 1 (2007).
9. T. Erneux, G. Hek, M. Yousefi, and D. Lenstra, Proc. SPIE **5452-44**, 303 (2004).
10. K. Green and B. Krauskopf, Opt. Commun. **258**, 243 (2006).
11. M. Nizette and T. Erneux, Proc. SPIE **6184–32**, 61840W (2006).
12. H. Erzgräber, B. Krauskopf, D. Lenstra, A. Fischer, and G. Vermuri, "Feedback phase sensitivity of a semiconductor laser with filtered optical feedback," Phys. Rev. E (to be published).
13. K. Engelborghs, T. Luzyanina, and G. Samaey, Tech. Rep. TW-330 (Department of Computer Science, Katholieke Universiteit Leuven, 2001).
14. R. Szalai, G. Stépán, and S. J. Hogan, SIAM J. Sci. Comput. **28**, 1301 (2006).
15. B. Krauskopf, in *Unlocking Dynamical Diversity: Optical Feedback Effects on Semiconductor Lasers*, D. Kane and K. Shore, eds. (Wiley, 2005), pp. 147–183.